ELSEVIER

Applied Surface Science 7068 (2001) 1–8

applied surface science

www.elsevier.nl/locate/apsusc

The influence of chemical treatments on tungsten films found in integrated circuits

Scott S. Perry[a,*], Heather C. Galloway[b], Paul Cao[a], Evelynn J.R. Mitchell[b], Debbie C. Koeck[b], Christopher L. Smith[b], Min Soo Lim[a]

[a]*Department of Chemistry, University of Houston, Houston, TX 77204, USA*
[b]*Department of Physics, Southwest Texas State University, San Marcos, TX 78666, USA*

Received 4 December 2000; accepted 18 March 2001

Abstract

The influence of four different chemical solutions on the composition, morphology, and etch rates of thin, chemically vapor deposited tungsten films have been investigated. These films are the standard material patterned to create tungsten plugs in integrated circuits through a chemical mechanical planarization (CMP) step. The tungsten films were treated with aqueous solutions of KOH, $KIO_3 + NaOH$, $H_2O_2 + NH_4OH$, and $H_2O_2 + HCl$. We have evaluated the resulting changes in the surface chemical composition of the tungsten film with X-ray photoelectron spectroscopy (XPS). Changes in film morphology have been recorded with atomic force microscopy and material removal rates have been determined with calibrated four-point-probe resistivity measurements. Together, these measurements demonstrate the complex manner in which chemical pre-treatments in the CMP process influence thin tungsten films. © 2001 Published by Elsevier Science B.V.

PACS: 81.65.Cf

Keywords: Tungsten; Tungsten oxide; Chemical mechanical planarization; Chemical mechanical polishing; X-ray photoelectron spectroscopy; Atomic force microscopy

1. Introduction

The ability to fabricate integrated circuit components on increasingly smaller length scales is the basis of the continued state of advancement within the microelectronics industry. The shrinking scale of the devices allows an increase in the density of components yet also requires an increase in the need for multiple level metal interconnects. To date, multiple levels of interconnects have only been realized through global planarization or polishing techniques. This approach is also crucial to the industry's desire to increase the size of the wafers being fabricated, in order to allow more circuits to be manufactured simultaneously, and to accommodate the decrease of focal depth of optical lithography needed to produce smaller lateral dimensions. Chemical mechanical planarization (CMP) has become an enabling technology in these areas for the microelectronics industry. Past successes in CMP have been based largely upon empirical data that has allowed individual manufacturers to optimize proprietary techni-

* Corresponding author. Tel.: +1-713-743-2715; fax: +1-713-743-2709.
E-mail address: perry@uh.edu (S.S. Perry).

0169-4332/01/$ – see front matter © 2001 Published by Elsevier Science B.V.
PII: S0169-4332(01)00308-7

ques. As smaller device dimensions press the limits of current planarization technology, knowledge of the fundamental chemical and mechanical mechanisms of CMP are necessary to meet industry requirements. A more complete understanding of the fundamental steps of the process also will provide the opportunity to design new planarization techniques as new materials are introduced to devices.

Although tungsten CMP would seemingly be well understood in terms of the fundamental mechanisms due to its widespread use throughout the industry, uncertainty regarding the role of the chemical nature of the interface throughout the pre-clean and polishing sequence still exists. In particular, the existence and importance of a surface oxide layer remains a subject of active investigation [1–8]. An early mechanism for CMP proposed by Kaufmann et al. [9] suggested that the presence of an oxide protected low areas from corrosion during CMP. However, more recent work by Stein et al. [5–7] has been interpreted to mean that a passive oxide layer is not present during the polishing step even if an oxide layer is formed by ambient or liquid exposure prior to polishing. These differing views of foundational issues such as surface composition highlight the need for further studies of the fundamental aspects of CMP processes.

Tungsten CMP is typically carried out in acidic solutions using an oxidizing agent and abrasive particles. Both the chemical and physical character of the tungsten surface can be influenced by the individual components of the abrasive slurry. The complex nature of the polishing solution as well as the potential for both chemical (oxidation, reduction, dissolution) and physical (adhesion, friction, fracture, plowing) interactions require model studies of the interface to be carried out in order to delineate the individual roles of the different components and interactions.

In the work reported here, we have examined four chemical treatments found in the pre-cleaning or etching steps of tungsten CMP [1,2,10]. The purpose of this study has been to identify the chemical effects on the tungsten surface and to establish patterns of surface reactivity in the absence of any mechanical action. These studies have involved exposing chemically vapor deposited tungsten films to aqueous solutions of KOH, $KIO_3 + NaOH$, $H_2O_2 + NH_4OH$, and $H_2O_2 + HCl$ for short amounts of time. Following the aqueous treatments, the resulting changes in the chemical composition of the tungsten film have been measured ex situ with X-ray photoelectron spectroscopy (XPS). This work demonstrates that a range of oxide compositions can be produced at the W-surface, varying in both tungsten oxidation state and oxide film thickness. In addition, physical changes in the tungsten film morphology have been recorded with atomic force microscopy. Finally, the physical and chemical changes have been correlated with material removal rates measured with calibrated four-point-probe resistivity measurements. The results of these measurements demonstrate the complex manner in which chemical treatments can influence thin tungsten films and are discussed in terms of the surface properties related to CMP.

2. Experimental

Tungsten films were provided by Lucent Technologies and were deposited by chemical vapor deposition on 8 in. wafers, which in turn were diced into smaller samples for these studies. In the deposition process, a 10 000 Å SiO_2 layer was formed on the single crystal silicon wafer and was then followed by the growth of a 200 Å thick Ti/TiN barrier layer. An initial 500 Å tungsten seed layer was deposited through the reaction of $WF_6 + SiH_4 + H_2 + Ar$, while the final tungsten layer (∼4000 Å) was deposited through the reaction of $WF_6 + H_2 + Ar$ at a temperature of 425°C and a pressure of 40 Torr. Prior to solution treatment, the tungsten films were solvent cleaned using alternate treatments of ethanol, acetone, and distilled deionized water and dried under a stream of pure nitrogen gas. Aldrich reagent grade chemicals or better, diluted in deionized 18 MW water, were used in all instances. Although the use of organic solvents is known to result in a residual hydrocarbon layer, the above procedure was employed to standardize the preparation of the tungsten surfaces.

The tungsten films were chemically treated in four different solutions for specified durations: (i) a mixture of 4.0×10^{-3} M $HCl + 0.1$ M H_2O_2 (pH = 2.4) for 5 min, (ii) a mixture of 3.2×10^{-3} M NH_4OH and 0.1 M H_2O_2 (pH = 11.0) for 5 min, (iii) a mixture of 0.1 M KIO_3 and 1.0 M NaOH (pH = 14) for 1 min, and (iv) 0.1 M KOH (pH = 13) for 5 min. Following

these solution treatments, the tungsten films were dried under pure nitrogen and transferred to the vacuum chamber for surface analysis. All samples experienced the identical, brief exposure to ambient conditions, potentially resulting in the slight reoxidation of the chemically treated surface or the adsorption of hydrocarbon species, yet did not preclude an understanding of the influence of the different chemical treatments.

XPS measurements were made using a PHI 5750 ESCA system equipped with a standard Al X-ray source (Kα, 1486.6 eV). Each of the solution-treated surfaces was analyzed without further treatment in vacuum. A low-flux, low energy ion gun was used during data collection to circumvent sample charging; however, this did not alter the surface composition. Survey spectra were collected from each surface and confirmed the presence of only tungsten, oxygen, and carbon at the surface. High resolution core level spectra were collected from the tungsten 4f, oxygen 1s, and carbon 1s regions with a 0.1 eV energy step and at a pass energy of 23.50 eV. A flux of lower energy ions and electrons at the sample surface prevented surface charging during the course of XPS measurements. Integrated intensities of these regions were normalized using published sensitivity factors and used to calculate the percent atomic concentrations of the surface region [11]. Distributions in the oxidation state of the tungsten surface species were evaluated by deconvolution of the tungsten 4f region. This procedure made use of published spectral data [8,12–19], a mixed Gaussian–Lorentzian peak shape, and in all cases maintained the same full-width half-maximum and energy splitting between the $4f_{7/2}$ and $4f_{5/2}$ peaks.

The surface morphology of the tungsten films was evaluated using atomic force microscopy before and after solution treatment and a nitrogen drying step. These measurements were performed using a Park AutoProbe CP with silicon cantilevers having a nominal tip radius of ∼200 Å (according to manufacturer's specifications). All images were collected as a spatial map of the normal cantilever deflection. Cross-sectional plots of the images represent the deflection of the cantilever normal to the surface plane as function of distance across one horizontal line of the image (obtained through the top-to-bottom center of the image unless otherwise noted).

Finally, the relative etch or material removal rates of the four different solutions have been evaluated by measuring the average film thickness before and after exposure to the individual solution treatments (in the absence of mechanical action). Film thickness has been determined through four-point-probe resistance measurements in the following manner. Film thickness was calibrated using cross-sectional scanning electron microscopy (SEM) [20] both before and after a chemical treatment and these results were compared to the four-point-probe measurements. The initial average tungsten film thickness across the entire wafer was 4600 ± 200 Å. Using a four-point-probe measurement, the resistance of the film was measured. The four-point-probe apparatus utilized in-line contacts to the sample and applied a known current to the film through the outside two probes. The current in our system was applied alternately in both directions at a switching frequency of 17 Hz (by application of a square wave source). The voltage difference produced between the two inner probes was measured with a lock-in amplifier operating at the same frequency, ensuring that the measured voltage difference is due to the applied current. This method is inherently impervious to the influence of contact and spreading resistances and allowed the determination of the direct relationship between film resistance and film thickness [21,22]. Initial film resistivity was ∼9.8 μΩ cm (as compared to the bulk value for W of 5.6 μΩ cm) and was assumed to remain constant throughout the film. The specific thickness values were then converted to material removal rates by accounting for the etch time.

3. Results

Five tungsten films were analyzed with XPS to determine the chemical composition of the surface region. These samples included the as-received tungsten film (rinsed with organic solvents), and four additional tungsten films treated with the solutions described in Section 2. Each of the surface regions of the films contained an appreciable amount of carbon (non-carbidic). However, this is believed to be the result of the adsorption of adventitious carbon from the laboratory atmosphere. Depth profile studies of the untreated tungsten film performed elsewhere con-

Table 1
Composition of tungsten films following different chemical treatments

Sample	Normalized O/W-values	WO_x (%)	Material removal rate (Å/min)
As-received	2.10	44.5	–
$NH_4OH + H_2O_2$	1.20	35.8	352 ± 35
$HCl + H_2O_2$	1.35	40.3	49 ± 25
KIO_3 + NaOH	1.61	44.8	27.0 ± 15
KOH	0.95	28.7	<10

firmed that there was little carbon (<1%) within the [20]. Although the amount of carbon was observed to vary from sample to sample, we do not believe that relative differences in the amount of carbon have significantly influenced the quantitative results presented for oxygen and tungsten concentrations. The results of these concentration measurements are recorded in Table 1 as the ratio of oxygen-to-tungsten (O/W) present in the total integrated surface region. As previously described, these values were obtained through integration of high resolution O 1s and W 4f regions and correction for differing sensitivity factors [12].

The resulting composition of the surface regions following chemical treatment was further assessed through deconvolution of the peaks present in the tungsten 4f core level spectra. A representative spectrum of the W 4f region collected from the as-received tungsten film is shown in Fig. 1. In this spectrum, four peaks are apparent and are assigned to the $4f_{7/2}$ and

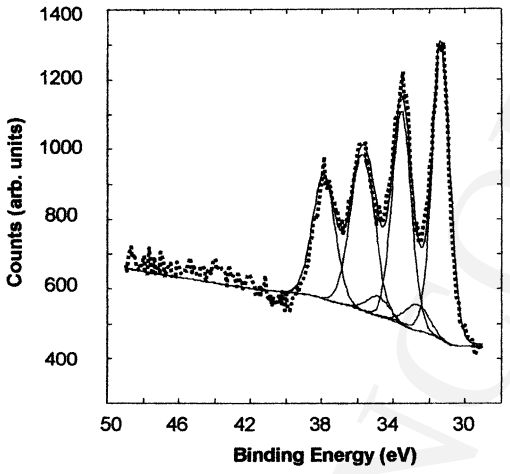

Fig. 1. Tungsten 4f XPS spectrum of the as-received tungsten film following a solvent rinse.

$4f_{5/2}$ of metallic tungsten (W^0) and of tungsten in the +6 oxidation state, presumably in the form of WO_3. Further deconvolution of the spectrum revealed the presence of a third pair of peaks assigned to the 4f doublet arising from tungsten in the +4 oxidation state, again presumably in the form of WO_2. The binding energy values and peak splittings for each of the doublets were consistent with values found in [8,13–19] and were reproducible within all the spectra of this study, as presented in Table 2. Integration of the deconvoluted spectra produced a measure of the distribution of oxidation states throughout the surface region; relative values determined from the $4f_{7/2}$ peaks are presented in Table 3.

For the as-received tungsten films, these data indicate that ∼44% of the tungsten within the surface region exists in an oxidized form (Table 1). The clear presence of metallic tungsten (W^0) suggests the physical picture of a thin tungsten oxide layer existing over the bulk metallic film. We acknowledge here the unlikelihood of finding all tungsten atoms of an amorphous oxide film in discrete oxidation states; however, we find that the model of discreet oxides (WO_2 and WO_3) fits the data reasonably well and provides a quantitative means for comparing the composition of the tungsten surface following various chemical treatments.

A similar analysis was performed for the tungsten films treated with the solutions described in Section 2. Distinct changes were observed in each of the spectra and could be accounted for, in terms of changes in the distribution of oxidation states through deconvolution procedures. The W 4f spectrum of the film treated with a solution of sodium hydroxide and potassium iodate is representative of the intensity shifts observed in the spectra of the treated surfaces and is shown in Figs. 2 and 3. Here the raw data is shown as a dotted line while the individual peaks used to fit the spectrum and their

Table 2
XPS binding energy of tungsten $4f_{7/2}$ peaks in different oxidation states

Compound	W-metal (W^0)	WO_2 (W^{4+})	WO_3 (W^{6+})
Measured binding energy (eV) of W $4f_{7/2}$	31.4 ± 0.1	32.5 ± 0.2	35.6 ± 0.2
References	[8–13,15,16]	[11–13]	[8,11–16]

Table 3
Composition of tungsten oxide components following different chemical treatments

Sample	W^0 (%)	W^{4+} (%)	W^{6+} (%)
As-received	55.5	6.3	38.2
$HCl + H_2O_2$	64.2	18.4	17.4
$NH_4OH + H_2O_2$	59.7	21.9	18.4
KIO_3 + NaOH	55.2	23.4	21.4
KOH	71.3	15.3	13.4

sum are shown as solid lines. Integrated values obtained from this treatment, as well as from similar treatments of data collected from the other surfaces, are reported in Table 3. From these data, the relative concentration of oxidized tungsten within the surface region was calculated (Table 1).

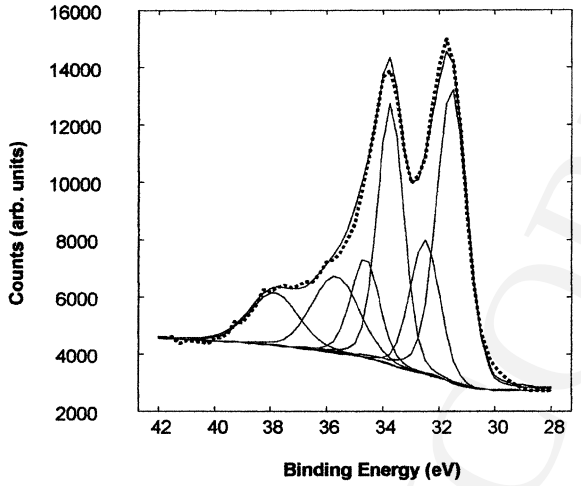

Fig. 2. XPS spectrum of the tungsten 4f region following a treatment of KIO_3 (0.1 M) + NaOH (1.0 M) for 1 min. The deconvolution procedure indicates little change in the total percentage of oxidized tungsten, but a dramatic shift in intensity from W^{6+} to W^{4+}, relative to the native oxide.

In addition to the changes in surface composition, we have investigated the relative rates of material removal for the different solutions. The etching process of the tungsten film occurs primarily through the dissolution of the interfacial tungsten oxide layer. As described in Section 2, material removal rates have been determined by four-point-probe resistivity measurements. This analysis is based on the principle that the measured electrical resistance of a film, which is much thinner than it is wide, will scale with thickness in a linear fashion. The four-point-probe method is inherently insensitive to contact and spreading resistance effects. With this method, we measured the removal rates of the four solutions over a range of immersion times. The rate of material removal was determined from the slope of the plot of thickness reduction versus immersion time. The results are

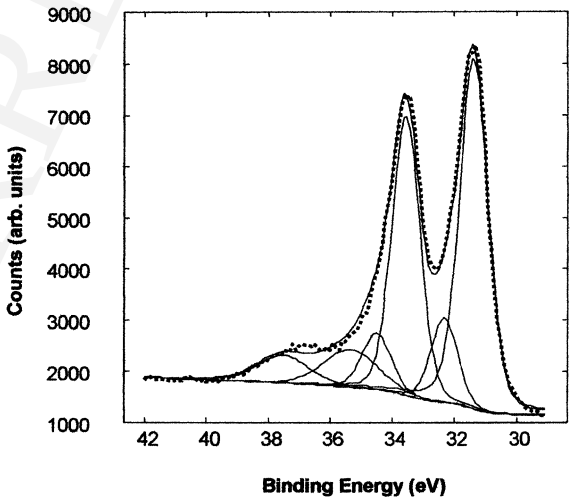

Fig. 3. XPS spectrum of the tungsten 4f region following a treatment of 0.1 M KOH for 5 min. Deconvolution of the spectrum indicates a strong reduction in the percentage of W that is oxidized as well as a shift in intensity from W^{6+} to W^{4+}.

presented in Table 1. Material removal rates varying by more than order of magnitude were observed, with the NH_4OH/H_2O_2 solution exhibiting the highest removal rate. The KOH solution exhibited the lowest rate of material removal.

Finally, the surface topography of the tungsten films has been measured with AFM both before and after solution treatments. Contact mode AFM images of the samples have provided an estimate of grain size as well as a quantitative measure of surface roughness. Here, surface roughness values are cited as the rms deviation of pixel heights from a best-fit plane through the image. As contact mode images are often convoluted with the shape of the probe tip, only sets of measurements performed with the same tip are presented to avoid artifacts due to tip-effects. Furthermore, we have insured that tip wear has not contributed to the observed effects by sequentially imaging as-received and treated surfaces with the same tip. The surface topography of the as-received film is shown in Fig. 4(a) and is characterized by an rms surface roughness of 150 ± 2 Å when measured over a $5\,\mu m \times 5\,\mu m$ area. For the tungsten films exposed to solutions of $HCl + H_2O_2$, $NaOH + KIO_3$, and KOH, little influence on the surface topography was observed. In contrast, a topographic image of the tungsten film following exposure to $NH_4OH + H_2O_2$ (Fig. 4(b)) clearly reveals that this

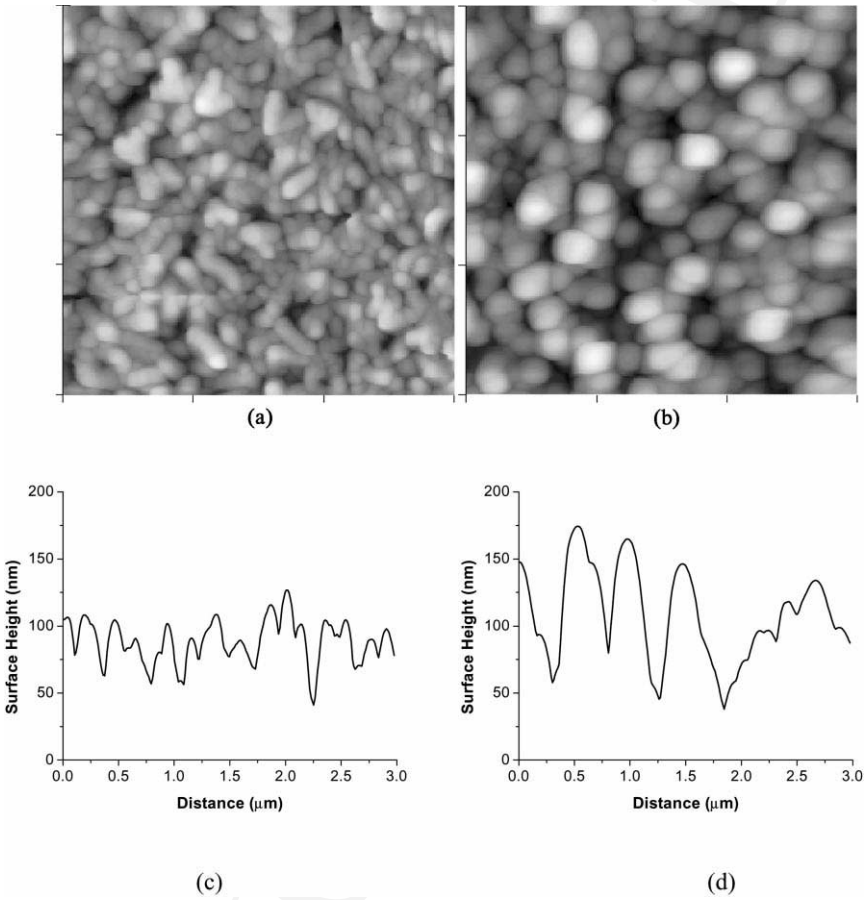

Fig. 4. (a) AFM image of the W-surface "as-received" taken in contact mode. The image is $3\,\mu m \times 3\,\mu m$. (b) An image of the W-surface after treatment in $NH_4OH + H_2O_2$ acquired under the same conditions. There is a significant change in the observed feature size from ~0.2 to ~0.4 μm. Respective cross-sectional topographic plots for the two surfaces are shown in (c) and (d), respectively. The plots represent the topographic height as a function of distance across the centerline (top-to-bottom) of the two images. The data have been artificially offset to be at the same height for purposes of comparison.

treatment results in a noticeable difference in the revealed 'grain' size. This observation is not simply the result of a greater amount of material being removed, as topographic studies of the etching process using the other solutions for proportionately longer times indicated little change in surface morphology. While the $NH_4OH + H_2O_2$ treatment did not produce a change in the rms surface roughness, cross-sectional topographic plots clearly indicate that a significant restructuring of the surface layer has occurred.

4. Discussion

The results presented above demonstrate that chemical treatments found in the cleaning and polishing steps of CMP can alter the tungsten surface a number of ways. First, these results clearly indicate that the chemical composition of the surface region is altered from that of the native oxide found on tungsten. This change is manifest in one of two fashions. In some cases, there is a net reduction in the thickness of the oxide. This is seen by comparing the oxygen-to-tungsten ratios or the WO_x (%) in the surface region of the chemically treated films to those of the native oxide (we note that the calculation of the percent oxidized tungsten neglects the carbon found in the surface region, since carbon is not present in a carbidic form, we do not believe that it affects the comparison of tungsten to tungsten oxide species). Of the four solutions investigated, the $HCl + H_2O_2$ and KOH solutions demonstrated the greatest chemical reduction of the oxide film (different from material removal) (Table 3). The combination of a basic solution with an oxidizing agent, which was observed to etch the tungsten surface (Table 1), did not substantially alter the thickness of the resulting oxide film, as judged from the integrated intensity of the W^0-peaks (Table 3). This observation points to the multifunctional role of solutions containing more than one active component.

While only certain solutions reduce the thickness of the oxide, all chemical treatments are observed to alter the composition of the oxide. This is clearly seen in the data of Table 3 and Figs. 1 and 2. Whether a cleaning or etching solution, a significant shift from W^{6+} to W^{4+} is observed. For the two treatments observed to reduce the oxide thickness, a corresponding increase in the metallic W^0-state is also observed. Regardless of film thickness, a fairly narrow range of compositions of the oxide is reached, with approximately equal amounts ($\pm 5\%$) of tungsten existing in the +4 and +6 oxidation states. Because the tungsten films have been transported through an ambient environment before the XPS measurements were performed and likely have been partially oxidized, it is not possible to conclude the exact composition of the surface regions under the different aqueous solutions. However, it is evident that all of the solutions investigated in this study dramatically alter the composition through the reduction of the oxide layer. The differences in film thickness, as well as the slight variations in oxide composition support the claim that this compositional analysis is not dramatically influenced by the reoxidation of tungsten in being transferred from an aqueous solution to the vacuum analysis system. The compositional results presented here are comparable to those of Kneer et al. [3] where changes in the surface stoichiometry of W-films were reported as a function of exposure to pH 2 and 4 solutions of KNO_3 and with the results of Tamboli et al. [8] where the films are electrochemically treated with H_2O_2 or KIO_3 solutions. The results presented above serve to delineate the influence of a number of individual treatments and, together with the etch rate measurements described below, to portray the influence of solution pH and oxidizing strength.

Two additional interfacial properties have been monitored with respect to the activity of these solutions in a CMP setting. These include the rate of material removal as well as the changes in surface morphology induced by the solution treatment. A survey of the results reported in Tables 1 and 3, together with the result that only the $NH_4OH + H_2O_2$ solution substantially altered the surface morphology, demonstrates that the activity of the solution components is affected by their combination with other species. Specifically, the combination of ammonium hydroxide and hydrogen peroxide acts to both dissolve and reform tungsten oxide layers at a rate much greater than the other solutions. The etch rate for this solution is approximately seven times greater than the highest of the other solutions ($HCl + H_2O_2$), as determined by four-point-probe measurements. This result, in combination with the

effective increase in feature size observed through AFM measurements, suggests that this surface undergoes substantial and simultaneous oxidation as well as oxide removal. While these data illustrate the complex influence of chemical treatments on tungsten films, they do not provide atomic level insight into the stepwise mechanisms of the process.

The process of CMP relies upon the precise control of solution chemistry and the resulting surface composition. The ultimate goal of this process is the production of a uniform, planar surface. For tungsten surfaces, the studies presented in this paper document three important phenomena, which likely contribute to the cleaning and etching of the surface. They include the reduction of the native surface oxide, the dissolution of tungsten oxide species, and the change in surface morphology. In situ studies are currently underway to follow changes in topographic and frictional properties under polishing conditions as a function of solution pH and oxidizing strength.

5. Conclusions

The influence of four aqueous solutions of varying pH and oxidizing strength on thin tungsten films has been measured in the absence of any mechanical motion with an array of surface analytical probes. Through this set of measurements, changes in surface composition and morphology, as well as variations in material removal rates have been observed for this series of solutions. Specifically, each solution acted to reduce the native surface oxide, decreasing the concentration of W^{6+}-species and relatively increasing the concentration of W^{4+}-species. In addition, each solution demonstrated the ability to etch the surface, although a substantial range of material removal rates was observed. The $NH_4OH + H_2O_2$ solution exhibited the largest removal rate and the greatest effect on the surface morphology. The changes in surface morphology produced by this solution and revealed by AFM represent a spatially anisotropic etch process, selectively revealing larger grains at the tungsten interface. These finding highlight the multiple and complex phenomena active in any chemical treatment of the surface and the importance of the specific solution composition in determining the net influence of the chemical treatment.

Acknowledgements

This work was supported by the Texas Higher Education Coordinating Board — Advanced Technology Program, Grant no. 003652-0041-1999. Tungsten CVD film samples were grown by Lucent Technologies, Orlando, FL. HCG also would like to acknowledge support from Research Corporation's Cottrell College Science Fund.

References

[1] C. Raghunath, K.T. Lee, E.A. Kneer, V. Mathew, S. Raghavan, Electrochem. Soc. Proc. 96 (22) (1996) 1.
[2] D.J. Stein, D.L. Hetherington, T. Guilinger, J.L. Cecchi, J. Electrochem. Soc. 145 (1998) 3190.
[3] E.A. Kneer, C. Raghunath, S. Raghavan, J. Electrochem. Soc. 143 (12) (1996) 4095.
[4] E.A. Kneer, C. Raghunath, V. Mathew, S. Raghavan, J. Electrochem. Soc. 144 (9) (1997) 3041.
[5] D.J. Stein, D.L. Hetherington, J.L. Cecchi, J. Electrochem. Soc. 146 (1999) 376.
[6] D.J. Stein, D.L. Hetherington, T. Guilinger, J.L. Cecchi, J. Electrochem. Soc. 146 (1999) 1934.
[7] D.J. Stein, D.L. Hetherington, T. Guilinger, J.L. Cecchi, J. Mater. Res. 14 (1999) 3695.
[8] D. Tamboli, S. Seal, V. Desai, J. Vac. Sci. Technol. A 17 (4) (1999) 1168.
[9] F.B. Kaufman, D.B. Thompson, R.E. Broadie, M.A. Jaso, W.L. Guthrie, D.J. Pearson, M.B. Small, J. Electrochem. Soc. 138 (1991) 3460.
[10] W. Kern, D.A. Poutinen, RCA Rev. 30 (2) (1970) 187.
[11] Anon., unpublished data.
[12] A. Katrib, F. Hemming, P. Wehrer, L. Hilaire, G. Maire, J. Elect. Spectrom. Rel. Phenom. 76 (1995) 195.
[13] A. Nyholm, A. Berndtsson, N. Märtensson, J. Phys. C: Solid State Phys. 13 (1980) L1091.
[14] T.E. Madey, C.-H. Nien, K. Pelhos, J.J. Kolodziej, I.M. Abdelrehim, H.-S. Tao, Surf. Sci. 438 (1999) 191.
[15] C. Cantalini, M.Z. Atashbar, M.K. Ghantasala, S. Santucci, W. Wlodarski, M. Passacantando, J. Vac. Sci. Technol. A 17 (4) (1999) 1873.
[16] C. Bigey, V. Logie, A. Bnsaddik, J.L. Schmitt, G. Maire, J. Phys. IV (France) 8 (1998) Pr5–553.
[17] C. Bigey, L. Hilaire, G. Maire, J. Catal. 184 (1999) 406.
[18] L. Su, Q. Dai, Z. Lu, Spectrochim. Acta: Part A 55 (1999) 2179.
[19] H.L. Zhang, D.Z. Wang, N.K. Huang, Appl. Surf. Sci. 150 (1999) 34.
[20] Data supplied by Lucent Technologies, Orlando, FL.
[21] D.K. Schroder, Semiconductor Material and Device Characterization, 2nd Edition, Wiley/Interscience, New York, 1998.
[22] W.E. Beadle, J.C.C. Tsai, R.D. Plummer, Quick Reference Manual for Silicon Integrated Circuit Technology, Wiley/Interscience, New York, 1985.